

Accepted Manuscript

Research paper

Slow Magnetic Relaxation in Two Octahedral Cobalt(II) Complexes with Positive Axial Anisotropy

Jianjun Zhou, Jinbo Song, Aihua Yuan, Zhenxing Wang, Lei Chen, Zhong-Wen Ouyang

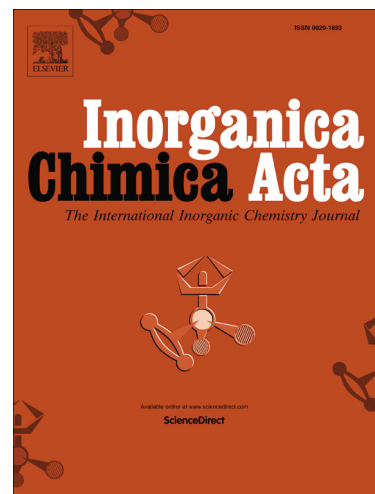
PII: S0020-1693(18)30329-3
DOI: <https://doi.org/10.1016/j.ica.2018.04.003>
Reference: ICA 18194

To appear in: *Inorganica Chimica Acta*

Received Date: 7 March 2018
Revised Date: 30 March 2018
Accepted Date: 3 April 2018

Please cite this article as: J. Zhou, J. Song, A. Yuan, Z. Wang, L. Chen, Z-W. Ouyang, Slow Magnetic Relaxation in Two Octahedral Cobalt(II) Complexes with Positive Axial Anisotropy, *Inorganica Chimica Acta* (2018), doi: <https://doi.org/10.1016/j.ica.2018.04.003>

This is a PDF file of an unedited manuscript that has been accepted for publication. As a service to our customers we are providing this early version of the manuscript. The manuscript will undergo copyediting, typesetting, and review of the resulting proof before it is published in its final form. Please note that during the production process errors may be discovered which could affect the content, and all legal disclaimers that apply to the journal pertain.



Slow Magnetic Relaxation in Two Octahedral Cobalt(II) Complexes with Positive Axial Anisotropy

Jianjun Zhou,^a Jinbo Song,^a Aihua Yuan,^{a,*} Zhenxing Wang,^{b,*} Lei Chen,^{a,*}

Zhong-Wen Ouyang^b

^a*School of Environmental and Chemical Engineering, Jiangsu University of Science and Technology, Zhenjiang 212003, China*

E-mail: aihua.yuan@just.edu.cn; chenlei@just.edu.cn

^b*Wuhan National High Magnetic Field Center & School of Physics, Huazhong University of Science and Technology, Wuhan 430074, China*

E-mail: zxwang@hust.edu.cn

Abstract: Two mononuclear Co(II) complexes [Co(L)₄(NO₃)₂] (L= 3-phenylpyrazole for **1** and 4-methylpyridine for **2**) featuring distorted octahedral geometry were prepared and structurally characterized by X-ray crystallographic analyses. Direct-current magnetic and high-frequency/field electron paramagnetic resonance measurements reveal that both complexes have the large and positive *D* values with the non-negligible transverse anisotropy (*E*). Slow magnetic relaxation effects were observed under the applied direct-current field in **1** and **2** by dynamic alternative-current magnetic susceptibility measurements, which provide two interesting examples of six-coordinate Co(II)-based single ion magnets constructed by nitrate groups and nitrogen heterocyclic compounds in mono-dentate coordination modes.

Keywords: Cobalt; magnetic properties; single-ion magnet; EPR spectroscopy

1. Introduction

The field of single molecule magnets (SMMs) based on single paramagnetic 3*d* ion has invoked much research,¹ and have been rapidly expanding over the past

several years since the first discovery of slow magnetic relaxation in four-coordinate Fe(II) complexes by Long *et al.*² These mononuclear SMM, also called single ion magnets (SIMs), include those of Cr(II),³ Mn(III),⁴ Fe(I),⁵ Fe(II),^{2,6} Fe(III),⁷ Co(II),⁸⁻¹³ Ni(I),¹⁴ Ni(II),¹⁵ Re(IV),¹⁶ Ir(IV)¹⁷, or Os(V)¹⁸ ions with various coordination number and in different coordination environments. The greatest attention has been devoted to the class of Co(II)-SIMs for its versatility of coordination polyhedron and large magnetic anisotropy. As is well-known, the symmetry of the coordination geometry plays a crucial role on enhancing the magnetic anisotropy for Co(II)-SIMs. For example, Mallah T. group systematically investigates magneto-structural relationship in mononuclear trigonal bipyramidal Co(II) complexes.^{10b,10h,10i}

In 2012, Vallejo *et al.* reported the first example of field-induced single molecule magnet behavior in a mononuclear six-coordinate Co(II) complex, *cis*-[Co^{II}(dmphen)₂(NCS)₂].0.25EtOH (dmphen = 2,9-dimethyl-1,10-phenanthroline) with distorted octahedron, which exhibits the positive axial magnetic anisotropy ($D = +98 \text{ cm}^{-1}$).^{11a} Subsequently, many mononuclear octahedral Co(II) complexes with slow magnetic relaxation were found.^{11b-11j} It is interesting to note that two possible signs of D values were reported for the Co(II) complexes with distorted octahedron geometry even though almost SIMs based on Co(II) with distorted octahedron geometry display the positive zero-field splitting parameter ($D > 0$) with only rare exceptions. For six-coordinate Co(II)-SIMs with trigonal prismatic geometry, a negative anisotropy was demonstrated.^{11k-11s} Zhu *et al.* observed zero-field slow magnetic relaxation for a series of Co(II) complex (HNEt₃)(Co^{II}Co^{III}₃L₆) (H₂L = *R*-4-bromo-2-((2-hydroxy-1-phenylethylimino) methyl)phenol) with only one paramagnetic Co(II) ion in distorted triangular prism geometry, which shows the large uniaxial magnetic anisotropy ($D < 0$).^{11k,11l} Novikov *et al.* have also reported a negative anisotropy ($D = -40 \text{ cm}^{-1}$) for a cobalt(II) cage complex with a trigonal prismatic coordination provided by the macrocyclic ligand. Recently, slow relaxation with the negative D values was observed in trigonal antiprismatic Co(II) complex.^{11o}

These reported results clearly show that the sign of zero-field splitting parameter is related to the coordinated geometry for these six coordinated Co(II) complexes.

Gomez-Coca *et al.*^{11c} predicted the six-coordinated high-spin system ($S = 3/2$), hexagon and pentagonal pyramid geometry correspond to the positive zero-field splitting parameter ($D > 0$), while trigonal prism geometry is consistent with the negative zero-field splitting parameter ($D < 0$). It should be also note-worthy that the reported six-coordinate Co(II) SIMs almost employs bidentate or multidentate N,O ligands, which provide the distortion caused by the chelate effect. Six coordinate Co(II)-SIMs with only mono-dentate ligand is rare. Therefore, the mono-dentate ligand concluding nitrate group and nitrogen heterocyclic compounds were employed to construct octahedral cobalt(II) complexes with large magnetic anisotropy, because these ligands exhibit very weak ligand field strength.^{12c,19,20} In this article, we report the syntheses, structures, and magnetic properties of two high-spin Co(II) complexes, $[Co(L)_4(NO_3)_2]$ ($L = 3$ -phenylpyrazole, **1**; 4-methylpyridine, **2**). Both complexes with the distorted octahedral geometry display the easy plane magnetic anisotropy ($D > 0$) and field-induce slow magnetic relaxation.

2. Experimental Section

2.1. General considerations

All manipulations were carried out using standard Schlenk techniques under nitrogen atmosphere. Solvents were dried over molecular sieves and distilled under nitrogen. Unless otherwise stated, all chemicals were purchased from commercial sources and used without further purification. The powder X-ray diffraction (PXRD) patterns for polycrystalline samples were measured at 298 K on a Bruker D8 Advance X-ray Diffractometer. The PXRD patterns confirm that all samples used for magnetic measurements and photoluminescence study are pure, corresponding with those simulated from single-crystal X-ray diffraction data, as shown in Figure S1 in supplementary material. Elemental analyses were performed on an Elementar Vario ELIII elemental analyzer.

2.2. Synthesis of $[Co(L)_4(NO_3)_2]$ ($L = 3$ -phenylpyrazole, **1**)

A solution of CoCl_2 (0.5 mmol, 0.065 g) in 10.0 mL ethanol was added to a solution of AgNO_3 (1.0 mmol, 0.17 g) in 10 mL ethanol. The mixture was stirred until the reaction was complete, then the insoluble silver chloride was removed by filtration. 3-phenylpyrazole (3.1 mmol, 0.48 g) was slowly added to the filtrate, and the solution was allowed to stand overnight. The brown block crystals of **1** were isolated in 68% yield based on Co content. Elemental analysis (%) calcd. for $\text{CoC}_{36}\text{H}_{24}\text{N}_{10}\text{O}_6$: C, 57.48; H, 3.19; N, 18.64. Found: C, 57.51; H, 3.18; N, 18.68.

2.3. Synthesis of $[\text{Co}(\text{L})_4(\text{NO}_3)_2]$ ($\text{L} = 4\text{-methylpyridine}$, **2**)

2 was prepared by the same procedure as compound **1**, but with 4-methylpyridine (3.10 mmol, 0.30 mL) used instead of 3-phenylpyrazole (3.1 mmol, 0.48 g). The red block crystals of **2** were isolated in 74% yield based on Co content. Elemental analysis (%) calcd. for $\text{CoC}_{24}\text{N}_6\text{O}_6\text{H}_{28}$: C, 51.90; H, 5.08; N, 15.13. Found: C, 50.97; H, 5.07; N, 14.91.

2.4. X-ray Structure Determination

X-ray diffraction data for **1** and **2** were collected using a Bruker APEX DUO diffractometer with a CCD area detector (Mo $\text{K}\alpha$ radiation, $\lambda = 0.71073 \text{ \AA}$).²¹ The collection for **1** and **2** were performed at $T = 296 \text{ K}$. The APEXII program was used for collecting frames of data, determining lattice parameters. Data were integrated through the SAINT. Absorption corrections were applied using SADABS.²² The structures were solved using SHELXS-2016 and subsequently completed by Fourier recycling using SHELXL-2016 program.²³ The Co atoms were firstly determined, and N and C atoms were subsequently identified by the difference Fourier maps. All non-hydrogen atoms were refined by anisotropic displacement parameters. Hydrogen atoms on organic ligands were set in the calculated positions and generated by the riding model. Crystallographic data, data collection, and refinement parameters for **1** and **2** are listed in Table S1 in the ESI.

2.5. Magnetic measurements

Direct-current (*dc*) magnetic susceptibility measurements were performed at fields up to 7 T between 1.8 and 300 K with a Quantum Design SQUID VSM magnetometer at 1 kOe (for **1**) and with a Quantum Design MPMS-XL17 SQUID instrument at 2 kOe (for **2**). Magnetization data were recorded from 1.8 to 5 K at fields up to 7.0 T. The temperature and frequency-dependent alternative-current (*ac*) susceptibility data using an oscillating *ac* field of 2.0 Oe and frequencies ranging from 1 to 1000 Hz for **1**, whereas an oscillating *ac* field of 5.0 Oe and frequencies ranging from 1 to 1500 Hz were used for **2**. The magnetic susceptibilities data were corrected for the sample holder, as well as for diamagnetism of the constituent atoms using Pascal's constants. High-frequency/field electron paramagnetic resonance (HF-EPR) measurements were performed on a locally developed spectrometer at the Wuhan National High Magnetic Field Center, using a pulsed magnetic field of up to 30 T.²⁴

3. Results and Discussion

The molecular structures of **1** and **2** were determined by their single-crystal X-ray diffraction analyses, which are shown in Figures 1 and 2. The crystallographic and structure refinement data and selected bond lengths and angles are listed in the Table S1 and S2. Both complexes **1** and **2** crystallize triclinic space group *P*-1. As shown in Figure 1, the central Co(II) ion in **1** shows a distorted octahedral coordinated geometry, in which the four nitrogen donor atoms of four 3-phenylpyrazole molecules form the equatorial plane, whereas the remaining oxygen atoms from two unidentate NO₃⁻ groups reside in the axial positions. In the equatorial plane, the Co–N distances are 2.125(2) and 2.103(2) Å, and the four equatorial N–Co–N angles between the neighboring N atoms are in the range of 87.80(9)°–94.48(10)°. The axial Co–O bond lengths (2.150(2) Å) are longer than the equatorial Co–N bonds, which implies that a distorted octahedron with pronounced elongation along the O3–Co–O3a bond due to the Jahn-Teller effect. All the angles formed by two diagonal atoms and the central Co ions are equal to the ideal value 180° in **1**.

For complex **2**, two crystallographically distinct molecules are present in an

asymmetric unit, featuring the different Co-X bonds lengths and X-Co-X angles (Figure 2). One axial ligand NO_3^- around Co2 atom is disordered, as depicted in Figure 2c. The equatorial Co-N bond lengths lie in ranges 2.136(4)–2.214(4) Å (Co1) and 2.140(4)–2.173(4) Å (Co2), while the axial Co-O bond lengths are 2.105(3)–2.111(3) Å for Co1 atom and 2.071(10)–2.185(13) Å for Co2 atom. The Jahn-Teller axes around Co are compressed along the O–Co1–O axes, although the distortion of O10 atom lead to the large Co2–O10 bond length (2.185(13) Å) and the short Co2–O10' bond length (2.121(3) Å). These Co–O and Co–N bond lengths in two complexes are consistent with the reported values.²⁵ The shortest distance of neighbouring Co(II) in **1** and **2** are 7.834 and 8.250 Å, respectively.

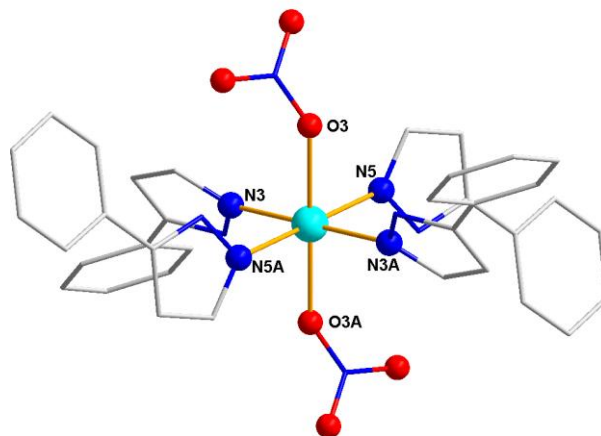


Figure 1. Molecular Structure of complexes **1**. H atoms are omitted for clarity.

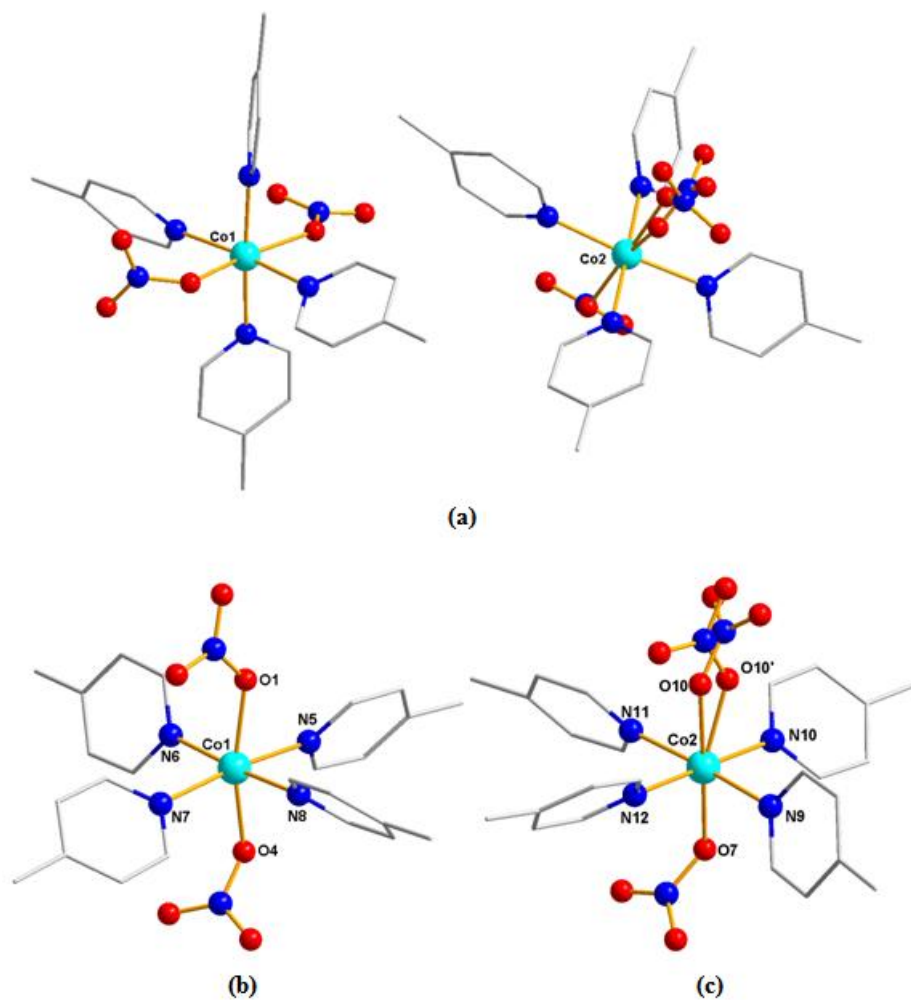
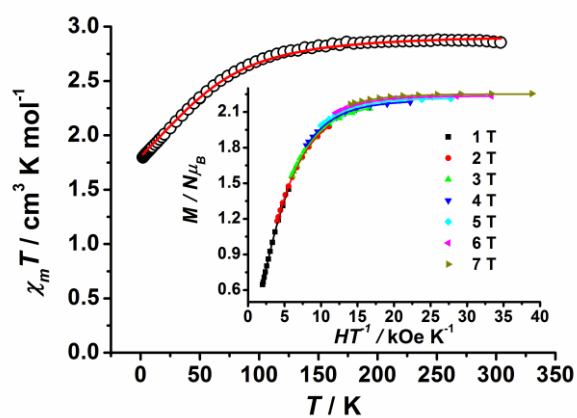


Figure 2. (a) Structure of the asymmetric unit in complex **2**; (b) Coordination structure for the Co1 atom in complex **2**. (c) Coordination structure for the Co2 atom in complex **2**. H atoms are omitted for clarity.



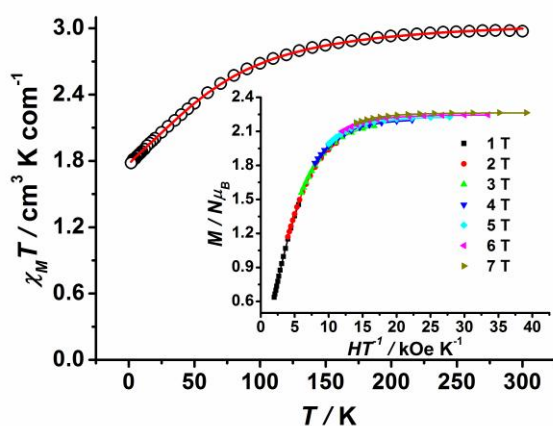


Figure 3. Variable-temperature dc susceptibility data of pure polycrystalline sample of **1** (top) and **2** (bottom). Inset: Variable-temperature, variable-field dc magnetization data collected in the range of 1.8-5 K between 1 and 7 T. Solid lines indicate the best fits with the *PHI* program.²⁶

Dc magnetic susceptibility data were collected in the temperature range from 1.8 and 300 K. As depicted in Figure 3, the values of $\chi_M T$ are 2.85 and 2.97 $\text{cm}^3 \text{K mol}^{-1}$ for **1** and **2** at room temperature, which are in agreement with one high-spin $d^7 \text{Co}^{\text{II}}$ ion ($S = 3/2$) with $g = 2.47$ and 2.52, respectively. The $\chi_M T$ products for **1** and **2** decrease very slightly as the temperature is lowered, until about 100 K where they drops precipitously to the final values of 1.80 and 1.78 $\text{cm}^3 \text{K mol}^{-1}$ at 1.8 K, respectively. This sudden drop can be attributed to the effect of magnetic anisotropy.

The field-dependent magnetizations for both complexes have been measured at 1.8 K in the range of 0-7 T (Figures S2 and S3). With the magnetic field increasing, the magnetizations continuously increase up to 2.33 and 2.26 $N\beta$ at 7 kOe for **1** and **2**, respectively, but do not reach the saturation, further suggesting the presence of a magnetic anisotropy and/or low-lying excited states in the system. Variable-temperature magnetization measurements for **1** and **2** were performed at fields ranging from 1 to 7 T and temperatures between 1.8 and 5 K (Figure 3 inset). The non-superposition of the M versus H/T plots also supports the presence of significant magnetic anisotropy in both complexes.

In order to probe the magnetic anisotropy, the magnetic susceptibilities and variable-temperature/field magnetization data were simultaneously modeled using the *PHI* program²⁶ to the spin Hamiltonian for one cobalt $S = 3/2$ ion with Zeeman

splitting and zero-field splitting. As depicted in Figure 3, the fittings are in general quite good. The best sets of parameters are listed in Table 1. The anisotropic g factor, the large and positive D values and the non-negligible E values were observed in **1** and **2**.

Table 1. The fitting results of the magnetization data by the *PHI* program¹⁸ for complexes **1** and **2**.

	$g_{x,y}$	g_z	D (cm ⁻¹)	$ E $ (cm ⁻¹)
1	2.55	2.35	71.4	13.0
2	2.50	2.70	71.5	9.8

To unambiguously know the sign of the magnetic anisotropy, HF-EPR measurements in the 60–350 GHz were performed at 4.2 K on the polycrystalline samples of **1** and **2** (Figures 4 and 5). All HF-EPR spectra show that three components consistent with an orbitally non-degenerate ground state, which is characteristic of a spin 3/2 system (high-spin Co^{II}) with large positive D values. Due to the large magnitudes of D values (71.4 and 71.5 cm⁻¹ obtained from the *dc* magnetic data for **1** and **2**) exceed the energy range in our measurement (350 GHz ~ 11.6 cm⁻¹), no transitions between the $m_S = \pm 1/2$ and $m_S = \pm 3/2$ were observed. The observed three components could be attributed to the intra-Kramers transitions within the $m_S = \pm 1/2$ manifold. The HF-EPR turning points at various microwave frequencies are extracted and plotted in Figure 5 as $2D$ map. Simulation of the representative HF-EPR spectra at 125 (**1**) and 120 GHz (**2**) and the field vs frequency data were performed to give the spin Hamiltonian parameters: $D = 72.9$ cm⁻¹ and $E = 8.9$ cm⁻¹ with $g_x = 2.45$, $g_y = 2.68$, $g_z = 2.03$ for **1**, and $D = 72.9$ cm⁻¹ and $E = 7.5$ cm⁻¹ with $g_x = 2.38$, $g_y = 2.60$, $g_z = 2.40$ for **2**. Although the derived magnitude of the ZFS parameters are not very precise, yet the large and positive D value has been unambiguously determined and is in agreement with the values obtained by the magnetization data, which further demonstrated the easy plane anisotropy for both complexes.

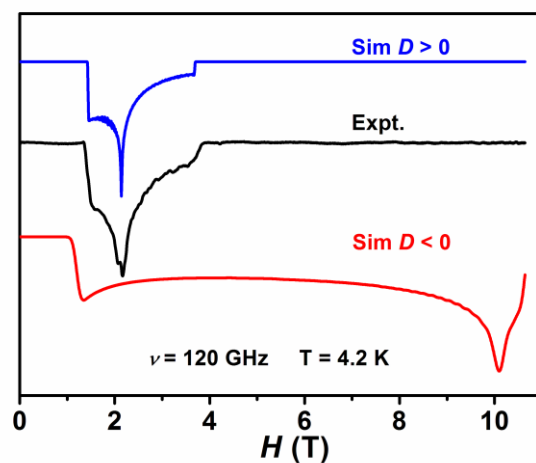
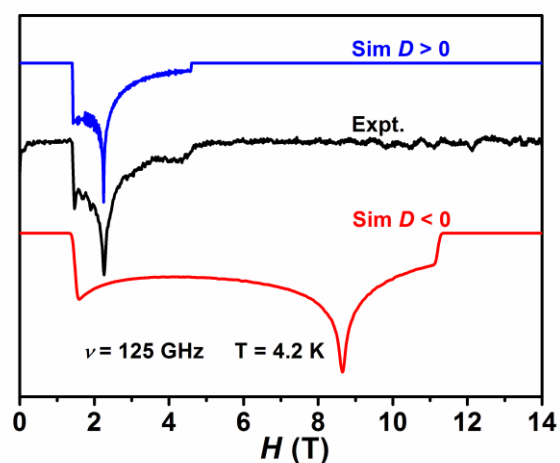


Figure 4. HF-EPR spectrum of **1** (top) and **2** (bottom) at 4.2 K and its simulations at 125 GHz for **1** and 120 GHz for **2**. The blue trace is spectrum simulated using the positive D value, while the red trace is the spectrum simulated using negative the D value, proving that **1** and **2** have positive D values. The spin Hamiltonian parameters used in the simulations were those obtained from the fits to the $2D$ field/frequency maps as in Figure 5.

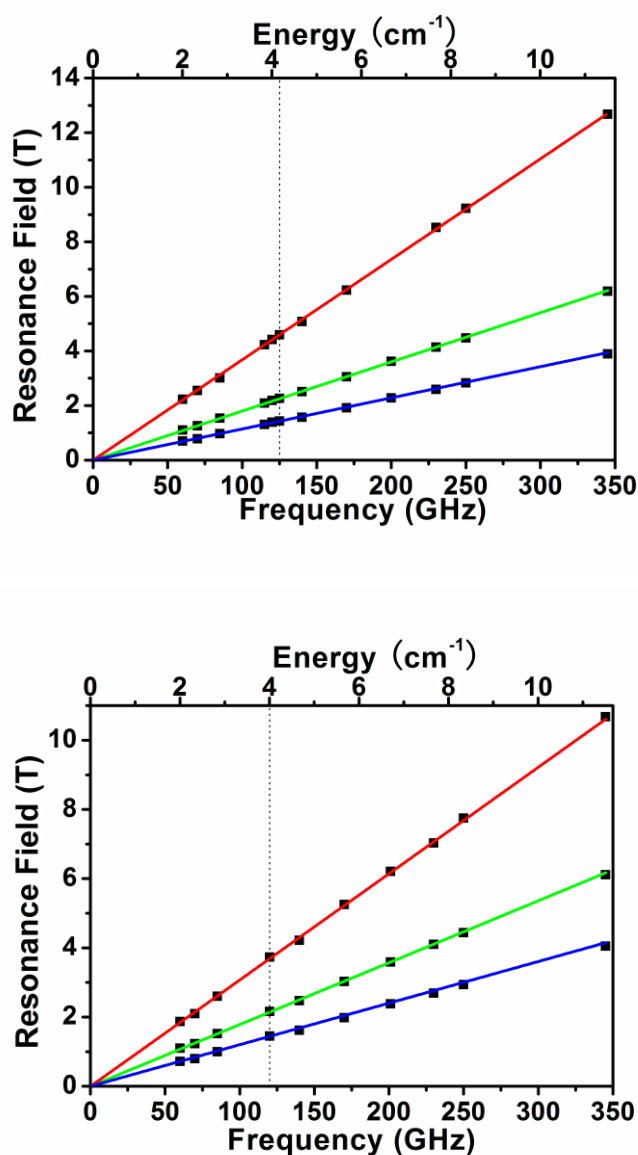


Figure 5. Resonance field vs microwave frequency (quantum energy) of EPR transitions for **1** (top) and **2** (bottom). Green, blue, and red curves are the simulations using the best-fitted spin Hamiltonian parameters with the magnetic field B parallel to the x , y , and z axes of the ZFS tensor, respectively. The vertical dashed line represents the frequency (125 GHz for **1** and 120 GHz for **2**) used in Figure 4 at which the spectra were recorded or simulated.

Frequency-dependent ac magnetic susceptibilities of **1** and **2** were performed at 1.8 K under different external dc fields (Figures S4 and S5). No slow magnetic relaxation is observed for two complexes under zero dc field. Upon an application of a small dc field, the peaks of χ_M'' signal for complexes **1** and **2** appear at 73.2 Hz and 760.2 Hz, respectively, which intensifies with the increasing of field. Thus, obviously the magnetic relaxation is slower in **1** than in **2**. It seems strange that the second hump

occurs in low frequency region and is small, when the applied dc field is increased. The small hump in low frequency region should be attributable to the weak intermolecular dipolar interactions. Although the long Co–Co distance implies the insignificant magnetic interactions between the spin ions, the dynamic magnetic properties could be influenced by the associated dipole-dipole interaction. This phenomenon was often observed in other SIMs based on lanthanide and 3*d* transition metal ions.^{11i,11o,27} To compare the dynamic magnetic properties of two complexes, additional ac magnetic susceptibility measurements were investigated using a dc field of 1000 Oe for **1** and 600 Oe for **2** at various temperatures (Figures 6 and S6–S7). As shown in Figure 6, both complexes showed a frequency dependence of χ_M'' signals. The frequency dependent χ_M'' peaks were observed for **1** at the temperature from 1.9 to 3.6 K, while at the temperature in the range of 1.9–2.5 K for **2**.

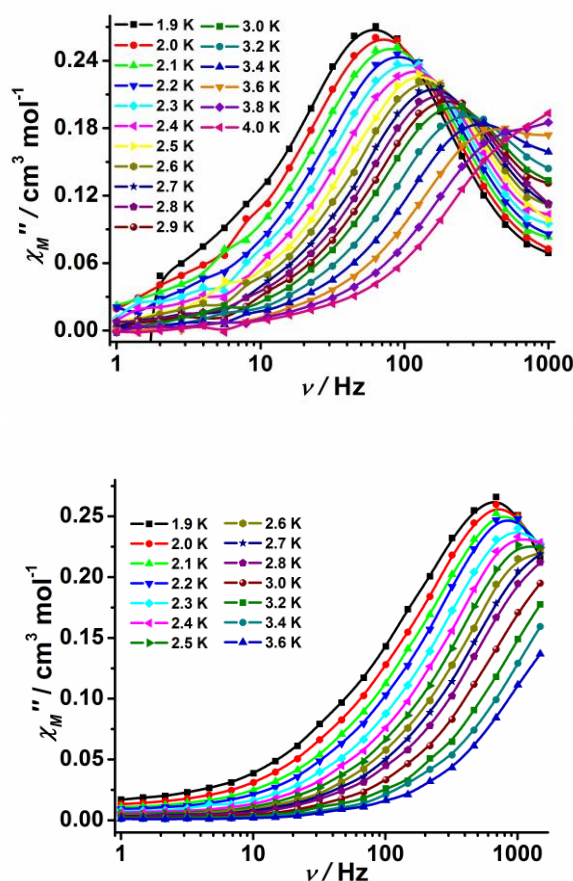


Figure 6. Frequency dependence of the out-of-phase *ac* magnetic susceptibility under applied dc field of 1000 Oe for **1** (top) and 600 Oe for **2** (bottom). The solid lines are for eye guide.

The relaxation times τ were evaluated from using the frequency of maxima in the frequency-dependent data, taking into account constructing the Arrhenius plots (Figure 7). The fit for the Arrhenius equation ($\tau = \tau_0 \exp(U_{\text{eff}}/k_B T)$) afforded the parameters of thermal energy barrier for magnetization relaxation (U_{eff}) and the pre-exponential factor (τ_0): $U_{\text{eff}} = 14.9$ K, $\tau_0 = 5.6 \times 10^{-6}$ s for **1**, and $U_{\text{eff}} = 7.3$ K, $\tau_0 = 6.8 \times 10^{-6}$ s for **2**. These results support the SMM behavior of **1** and **2**.

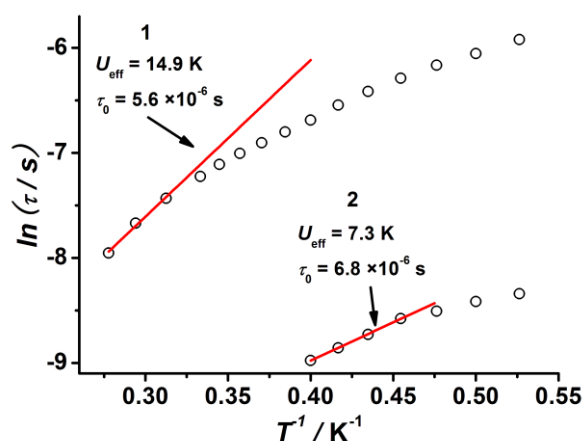


Figure 7. Relaxation time of the magnetization $\ln(\tau)$ vs T^{-1} plots for **1** and **2**. The solid lines represent Arrhenius fits.

It is notable that a Raman process makes significant contributions in most of the reported Co(II)-based SIMs with the octahedron and a direct one-phonon contribution should be not overlooked at low temperature. Therefore, we employed a model including direct and Raman relaxation mechanisms using the expression (1):

$$\tau^{-1} = AT + CT^n \quad (1)$$

The best fit was obtained with the following parameters: $A = 122.8 \text{ s}^{-1} \text{ K}^{-1}$, $C = 9.0 \text{ s}^{-1} \text{ K}^{-n}$ and $n = 4.3$ for **1**, and $A = 2071.6 \text{ s}^{-1} \text{ K}^{-1}$, $C = 0.7 \text{ s}^{-1} \text{ K}^{-n}$ and $n = 9.0$ for **2**. As depicted in Figures S8 and S9, the fit reproduce the experimental data very well (red solid line). Furthermore, it can be seen that the region at the entire temperature is almost dominated by the Raman process for **1**, whereas a direct process is the dominant process in the magnetic relaxation of **2**. It should be highlighted that the appreciable magnetic differences between the two complexes are caused by changing

the ligands of the equatorial plane.

4. Conclusions

In conclusion, we report the dynamic magnetic properties of two octahedral mononuclear Co(II) complexes $[\text{Co}(\text{L})_4(\text{NO}_3)_2]$ (L = 3-phenylpyrazole for **1**, and 4-methylpyridine for **2**). Analysis of their direct-current magnetic data and EPR spectroscopy reveals the easy plane magnetic anisotropy with large positive D values. Both complexes show field-induced slow magnetic relaxations, which is confirmed by alternating-current magnetic susceptibility measurements. However, the different relaxation processes of Raman and direct were observed in complexes **1** and **2**, respectively.

Acknowledgements

This work was supported by the National Natural Science Foundation (21601070, 51672114, 11774178, and 21701046), the China Postdoctoral Science Foundation (2016M601751), Jiangsu Planned Projects for Postdoctoral Research Funds (1601037B), and the Natural Science Foundation of the Higher Education Institutions of Jiangsu Province (16KJB150012).

Appendix A. Supplementary material

CCDC 1820114-1820115 contains the supplementary crystallographic data for complexes **1** and **2**. These data can be obtained free of charge via <http://www.ccdc.cam.ac.uk/conts/retrieving.html>, or from the Cambridge Crystallographic Data Centre, 12 Union Road, Cambridge CB2 1EZ, UK; fax: (+44) 1223-336-033; or e-mail: deposit@ccdc.cam.ac.uk.

Detailed crystallographic data and magnetic data of **1** and **2** are provided in Supplementary material. Supplementary data associated with this article can be found in the online version at doi: ???

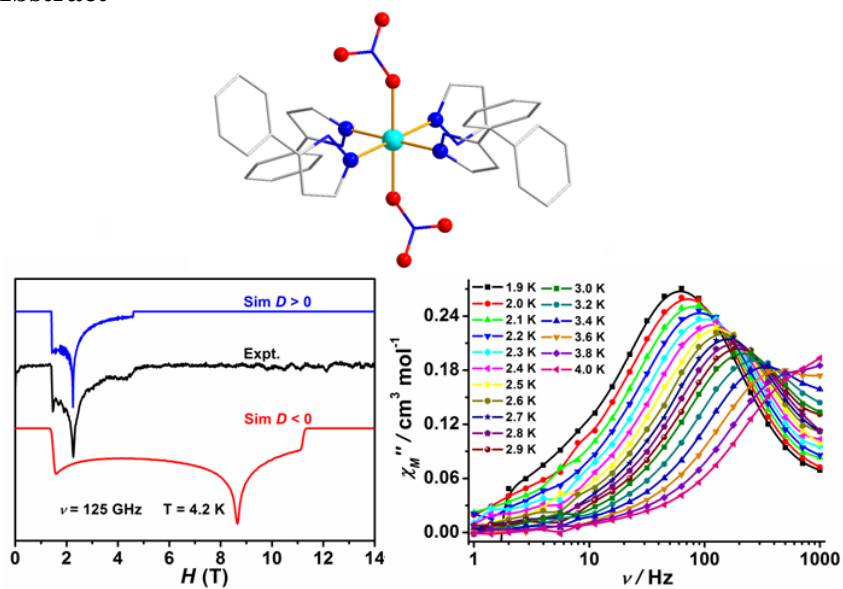
References:

- (1) (a) Craiga, G. A.; Murrie, M. *Chem. Soc. Rev.* **2015**, *44*, 2135. (b) Gómez-Coca, S.; Aravena, D.; Morales, R.; Ruiz, E. *Coordin. Chem. Rev.* **2015**, *289-290*, 379. (c) Bar, A. K.; Pichon, C.; Sutter, J. -P. *Coordin. Chem. Rev.* **2015**, *308*, 346.
- (2) Freedman, D. E.; Harman, W. H.; Harris, T. D.; Long, G. J.; Chang, C. J.; Long, J. R. *J. Am. Chem. Soc.* **2010**, *132*, 1224.
- (3) Cornia, A.; Rigamonti, L.; Boccedi, S.; Clérac, R.; Rouzières, M.; Sorace, L. *Chem. Commun.* **2014**, *50*, 15191.
- (4) (a) Ishikawa, R.; Miyamoto, R.; Nojiri, H.; Breedlove, B. K.; Yamashita, M. *Inorg. Chem.* **2013**, *52*, 8300. (b) Chen, L.; Wang, J.; Liu, Y. -Z.; Song, Y.; Chen, X. -T.; Zhang, Y. -Q.; Xue, Z. -L. *Eur. J. Inorg. Chem.*, **2015**, *2*, 271.
- (5) (a) Zadrozny, J. M.; Xiao, D. J.; Atanasov, M.; Long, G. J.; Grandjean, F.; Neese, F.; Long, J. R. *Nat. Chem.* **2013**, *5*, 577. (b) Samuel, P. P.; Mondal, K. C.; Sk, N. A.; Roesky, H. W.; Carl, E.; Neufeld, R.; Stalke, D.; Demeshko, S.; Meyer, F.; Ungur, L.; Chibotaru, L. F.; Christian, J.; Ramachandran, V.; Tol, J.; Dalal, N. S. *J. Am. Chem. Soc.* **2014**, *136*, 11964.
- (6) (a) Zadrozny, J. M.; Atanasov, M.; Bryan, A. M.; Lin, C. Y.; Recken, B. D.; Power, P. P.; Neese, F.; Long, J. R. *Chem. Sci.* **2013**, *4*, 125. (b) Harman, W. H.; Harris, T. D.; Freedman, D. E.; Fong, H.; Chang, A.; Rinehart, J. D.; Ozarowski, A.; Sougrati, M. T.; Grandjean, F.; Long, G. J.; Long, J. R.; Chang, C. J. *J. Am. Chem. Soc.* **2010**, *132*, 18115. (c) Lin, P. - H.; Smythe, N. C.; Gorelsky, S. I.; Maguire, S.; Henson, N. J.; Korobkov, I.; Scott, B. L.; Gordon, J. C.; Baker, R. T.; Murugesu, M. *J. Am. Chem. Soc.* **2011**, *133*, 15806. (d) Feng, X.; Mathonière, C.; Jeon, I.-R.; Rouzières, M.; Ozarowski, A.; Aubrey, M. L.; Gonzalez, M. I.; Clérac, R.; Long, J. R. *J. Am. Chem. Soc.* **2013**, *135*, 15880. (e) Bar, A. K.; Pichon, C.; Gogoi, N.; Duhayon, C.; Ramaseshac, S.; Sutter, J.-P. *Chem. Commun.* **2015**, *51*, 3616.
- (7) (a) Mossin, S.; Tran, B. L.; Adhikari, D.; Pink, M.; Heinemann, F. W.; Sutter, J.; Szilagy, R. K.; Meyer, K.; Mindiola, D. J. *J. Am. Chem. Soc.* **2012**, *134*, 13651. (b) Sato, R.; Suzuki, K.; Minato, T.; Shinoue, M.; Yamaguchi, K.; Mizuno, N. *Chem. Commun.* **2015**, *51*, 4081.
- (8) Eichhofer, A.; Lan, Y.; Mereacre, V.; Bodenstern, T.; Weigend, F. *Inorg. Chem.* **2014**, *53*, 1962.
- (9) (a) Zadrozny, J. M.; Liu, J. J.; Piro, N. A.; Chang, C. J.; Hill, S.; Long, J. R. *Chem. Comm.* **2012**, *48*, 3897. (b) Cao, D. K.; Feng, J. Q.; Ren, M.; Gu, Y. W.; Song, Y.; Ward, M. D. *Chem. Comm.* **2013**, *49*, 8863. (c) Buchholz, A.; Eseola, A. O.; Plass, W. C. *R. Chim.* **2012**, *15*, 929. (d) Yang, F.; Zhou, Q.; Zhang, Y. Q.; Zeng, G.; Li, G. H.; Shi, Z.; Wang, B. W.; Feng, S. H. *Chem. Comm.* **2013**, *49*, 5289. (e) Huang, W.; Liu, T.; Wu, D. Y.; Cheng, J. J.; Ouyang, Z. W.; Duan, C. Y. *Dalton Trans.* **2013**, *42*, 15326. (f) Zadrozny, J. M.; Telsler, J.; Long, J. R.; *Polyhedron* **2013**, *64*, 209. (g) Fataftah, M. S.; Zadrozny, J. M.; Rogers, D. M.; Freedman, D. E. *Inorg. Chem.* **2014**, *53*, 10716. (h) Cucos, P.; Tuna, F.; Sorace, L.; Matei, I.; Maxim, C.; Shova, S.; Gheorghe, R.; Caneschi, A.; Hillebrand, M.; Andruh, M. *Inorg. Chem.* **2014**, *53*, 7738. (i) Boča, R.; Miklovič, J.; Titiš, J. *Inorg. Chem.* **2014**, *53*, 2367. (j) Vaidya, S.; Upadhyay, A.; Singh, S. K.; Gupta, T.; Tewary, S.; Langley, S. K.; Walsh, J. P. S.; Murray, K. S.; Rajaraman, G.; Shanmugam, M. *Chem. Commun.* **2015**, *51*, 3739. (k) Carl, E.; Demeshko, S.; Meyer, F.; Stalke, D. *Chem. Eur. J.* **2015**, *21*, 1. (l) Cao, D. -K.; Wei, R. -H.; Li, X. -X.; Gu, Y. -W. *Dalton Trans.* **2015**, *44*, 5755. (m) Zadrozny, J. M.; Long, J. R. *J. Am. Chem. Soc.* **2011**, *133*, 20732. (n) Saber, M. R.; Dunbar, K. R. *Chem. Commun.* **2014**, *50*, 12266.
- (10) (a) Habib, F.; Luca, O. R.; Vieru, V.; Shiddiq, M.; Korobkov, I.; Gorelsky, S. I.; Takase, M. K.; Chibotaru, L. F.; Hill, S.; Crabtree, R. H.; Murugesu, M. *Angew. Chem., Int. Ed.* **2013**, *52*,

11290. (b) Ruamps, R.; Batchelor, L. J.; Guillot, R.; Zakhia, G.; Barra, A. -L.; Wernsdorfer, W.; Guihéry, N.; Mallah, T. *Chem. Sci.* **2014**, *5*, 3418. (c) Rajnák, C.; Titiš, J.; Fuhr, O.; Ruben, M.; Boča, R. *Inorg. Chem.* **2014**, *53*, 8200. (d) Nedelko, N.; Kornowicz, A.; Justyniak, I.; Aleshkevych, P.; Prochowicz, D.; Krupiński, P.; Dorosh, O.; Ślawska-Waniewska, A.; Lewiński, J. *Inorg. Chem.* **2014**, *53*, 12870. (e) Cruz, D. M. P.; Woodruff, D. N.; Jeon, I. -R.; Bhowmick, I.; Secu, M.; Hillard, E. A.; Dechambenoit, P.; Clérac, R. *New J. Chem.* **2014**, *38*, 3443. (f) Schweinfurth, D.; Sommer, M. G.; Atanasov, M.; Demeshko, S.; Hohloch, S.; Meyer, F.; Neese, F.; Sarkar, B. *J. Am. Chem. Soc.* **2015**, *137*, 1993. (g) Jurca, T.; Farghal, A.; Lin, P.-H. Korobkov, I.; Murugesu, M.; Richeson, D. S. *J. Am. Chem. Soc.* **2011**, *133*, 15814. (h) Cahier, B.; Maurice, R.; Bolvin, H.; Mallah, T.; Guihéry, N. *Magnetochemistry* **2016**, *2*, 31. (i) Shao, F.; Cahier, B.; Rivière, E.; Guillot, R.; Guihéry, N.; Campbell, V. E.; Mallah, T. *Inorg. Chem.* **2017**, *56*, 1104.
- (11) (a) Vallejo, J.; Castro, I.; Ruiz-García, R.; Cano, J.; Julve, M.; Lloret, F. De Munno, G.; Wernsdorfer, W.; Pardo, E. *J. Am. Chem. Soc.* **2012**, *134*, 15704. (b) Colacio, E.; Ruiz, J.; Ruiz, E.; Cremades, E.; Krzystek, J.; Carretta, S.; Cano, J.; Guidi, T.; Wernsdorfer, W.; Brechin, E. K. *Angew. Chem., Int. Ed.* **2013**, *52*, 9130. (c) Gomez-Coca, S.; Cremades, E.; Aliaga-Alcalde, N.; Ruiz, E. *J. Am. Chem. Soc.* **2013**, *135*, 7010. (d) Gómez-Coca, S.; Urtizberea, A.; Cremades, E.; Alonso, P. J.; Camón, A.; Ruiz, E.; Luis, F. *Nat. Comm.* **2014**, *5*:4300, 1. (e) Ion, A. E.; Nica, S.; Madalan, A. M.; Shova, S.; Vallejo, J.; Julve, M.; Lloret, F.; Andruh, M. *Inorg. Chem.* **2015**, *54*, 16. (f) Walsh, J.; Bowling, G.; Ariciu, A. -M.; Jailani, N.; Chilton, N.; Waddell, P.; Collison, D.; Tuna, F.; Higham, L. *Magnetochemistry* **2016**, *2*, 23. (g) Korchagin, D. V.; Pali, A. V.; Yureva, E. A.; Akimov, A. V.; Misochko, E. Y.; Shilov, G. V.; Talantsev, A. D.; Morgunov, R. B.; Shakin, A. A.; Aldoshin, S. M.; Tsukerblat, B. S. *Dalton Trans.* **2017**, *46*, 7540. (h) Valigura, D.; Rajnak, C.; Moncol, J.; Titis, J.; Boca, R. *Dalton Trans.* **2017**, *46*, 10950. (i) Li, J.; Han, Y.; Cao, F.; Wei, R. M.; Zhang Y. -Q.; Song, Y. *Dalton Trans.* **2016**, *45*, 9279. (j) Chen, L.; Zhou, J.; Cui, H. -H.; Yuan, A. -H.; Wang, Z.; Zhang, Y. -Q.; Ouyang, Z. -W.; Song, Y. *Dalton Trans.* **2018**, DOI: 10.1039/c7dt04651k. (k) Zhu, Y. -Y.; Cui, C.; Zhang, Y. -Q.; Jia, J. -H.; Guo, X.; Gao, C.; Qian, K.; Jiang, S. -D.; Wang, B. -W.; Wang, Z. -M.; Gao, S. *Chem. Sci.* **2013**, *4*, 1802. (l) Zhu, Y. -Y.; Zhu, M. -S.; Yin, T. -T.; Meng, Y. -S.; Wu, Z. -Q.; Zhang, Y. -Q.; Gao, S. *Inorg. Chem.* **2015**, *54*, 3716. (m) Zhu, Y. -Y.; Zhang, Y. -Q.; Yin, T. -T.; Gao, C.; Wang, B. -W.; Gao, S. *Inorg. Chem.* **2015**, *54*, 5475. (n) Novikov, V. V.; Pavlov, A. A.; Nelyubina, Y. V.; Boulon, M. E.; Varzatskii, O. A.; Voloshin, Y. Z.; Winpenny, R. E. *J. Am. Chem. Soc.* **2015**, *137*, 9792. (o) Zhang, Y. -Z.; Gómez-Coca, S.; Brown, A. J.; Saber, M. R.; Zhang, X.; Dunbar, K. R. *Chem. Sci.*, **2016**, *7*, 6519. (p) Peng, Y.; Bodenstein, T.; Fink, K.; Mereacre, V.; Ansona, C. E.; Powell, A. K. *Phys.Chem.Chem.Phys.* **2016**, *18*, 30135. (q) Peng, Y.; Mereacre, V.; Anson, C. E.; Zhang, Y. -Q.; Bodenstein, T.; Fink, K.; Powell, A. K.; *Inorg. Chem.* **2017**, *56*, 6056. (r) Pavlov, A. A.; Nelyubina, Y. V.; Kats, S. V.; Penkova, L. V.; Efimov, N. N.; Dmitrienko, A. O.; Vologzhanina, A. V.; Belov, A. S.; Voloshin, Y. Z.; Novikov, V. V. *J. Phys. Chem. Lett.* **2016**, *7*, 4111. (s) Ozumerzifon, T. J.; Bhowmick, I.; Spaller, W. C.; Rappéa, A. K.; Shores, M. P. *Chem. Commun.* **2017**, *53*, 4211.
- (12) (a) Huang, X. C.; Zhou, C.; Shao, D.; Wang, X. -Y. *Inorg. Chem.* **2014**, *53*, 12671. (b) Habib, F.; Korobkov, I.; Murugesu, M. *Dalton Trans.* **2015**, *44*, 6368. (c) Chen, L.; Chen, S. -Y.; Sun, Y. -C.; Guo, Y. -M.; Yu, L.; Chen, X. -T.; Wang, Z.; Ouyang, Z. W. ; Song, Y.; Xue, Z. -L. *Dalton Trans.* **2015**, *44*, 11482.

- (13) Chen, L.; Wang, J.; Wei, J. -M.; Wernsdorfer, W.; Chen, X. -T.; Zhang, Y. -Q.; Song, Y.; Xue, Z. -L. *J. Am. Chem. Soc.*, **2014**, *136*, 12213.
- (14) Poulten, R. C.; Page, M. J.; Algarra, A. G.; Le Roy, J. J.; López, I.; Carter, E.; Llobet, A.; Macgregor, S. A.; Mahon, M. F.; Murphy, D. M.; Murugesu, M.; Whittlesey, M. K. *J. Am. Chem. Soc.* **2013**, *135*, 13640.
- (15) Miklovič, J.; Valigura, D.; Boča, R.; Titiš, J. *Dalton Trans.* **2015**, *44*, 12484.
- (16) (a) Martnez-Lillo, J.; Mastropietro, T. F.; Lhotel, E.; Paulsen, C.; Cano, J.; De Munno, G.; Faus, J.; Lloret, F.; Julve, M.; Nellutla, S.; Krzystek, J. *J. Am. Chem. Soc.* **2013**, *135*, 13737. (b) Pedersen, K. S.; Sigrist, M.; Soensen, M. A.; Barra, A.-L.; Weyhermuller, T.; Piligkos, S.; Thuesen, C. A.; Vinum, M. G.; Mutka, H.; Weihe, H.; Clerac, R.; Bendix, J. *Angew. Chem. Int. Ed.* **2014**, *53*, 1351.
- (17) Pedersen, K. S.; Bendix, J.; Tressaud, A.; Durand, E.; Weihe, H.; Salman, Z.; Morsing, T. J.; Woodruff, D. N.; Lan, Y.; Wernsdorfer, W.; Mathonière, C.; Piligkos, S.; Klokishner, S. I.; Ostrovsky, S.; Ollefs, K.; Wilhelm, F.; Rogalev, A.; Clérac, R. *Nature Communications*, **2016**, *7*, 12195.
- (18) Pedersen, K. S.; Woodruff, D. N.; Singh, S. K.; Tressaud, A.; Durand, E.; Atanasov, M.; Perlepe, P.; Ollefs, K.; Wilhelm, F.; Mathonière, C.; Neese, F.; Rogalev, A.; Bendix, J.; Clérac, R.; *Chem. Eur. J.* **2017**, *23*, 11244.
- (19) Chen, L.; Zhou, J.; Yuan, A.; Song, Y. *Dalton Trans.* **2017**, *46*, 15812.
- (20) Ding, Y. -S.; Chilton, N. F.; Winpenny, R. E. P.; Zheng, Y. -Z. *Angew. Chem. Int. Ed.* **2016**, *55*, 16071.
- (21) SMART & SAINT Software Reference Manuals, version 6.45; Bruker Analytical X-ray Systems, Inc.: Madison, WI, **2003**.
- (22) Sheldrick, G. M. SADABS: Software for Empirical Absorption Correction, version 2.05; University of Göttingen: Göttingen, Germany, **2002**.
- (23) (a) Sheldrick, G. M. SHELXL97: Program for Crystal Structure Refinement; University of Göttingen: Göttingen, Germany, **1997**. (b) Sheldrick, G. M. *Acta Cryst.*, **2015**, *C71*, 3.
- (24) (a) Wang, S. L.; Li, L.; Ouyang, Z. W.; Xia, Z. C.; Xia, N. M.; Peng, T.; Zhang, K. B. *Acta Phys. Sin.* **2012**, *61*, 107601. (b) Nojiri, H.; Ouyang, Z. W. *Terahertz Sci. Technol.* **2012**, *5*, 1.
- (25) (a) Chen, Y.; Song, Y.; Zhang, Y.; Lang, J.-P. *Inorg. Chem. Commun.* **2008**, *11*, 572. (b) Hu, F. -L.; Mi, Y.; Gu, Y. -Q.; Zhu, L. -G.; Yang, S.-L.; Wei, H.; Lang, J. -P. *CrystEngComm* **2013**, *15*, 9553. (c) Hu, F. -L.; Wang, S. -L.; Wu, B.; Yu, H.; Wang, F.; Lang, J. -P. *CrystEngComm* **2014**, *16*, 6354. (d) Hu, F. -L.; Wu, W.; Liang, P.; Gu, Y. -Q.; Zhu, L.-G.; Wei, H.; Lang, J. -P. *Cryst. Growth Des.* **2013**, *13*, 5050.
- (26) Chilton, N. F.; Anderson, R. P.; Turner, L. D.; Soncini, A.; Murray, K. S. *J. Comput. Chem.* **2013**, *34*, 1164.
- (27) (a) Car, P. -E.; Perfetti, M.; Mannini, M.; Favre, A.; Caneschi, A.; Sessoli, R. *Chem. Commun.* **2011**, *47*, 3751. (b) Katoh, K.; Kajiwara, T.; Nakano, M.; Nakazawa, Y.; Wernsdorfer, W.; Ishikawa, N.; Breedlove, B. K.; Yamashita, M. *Chem. Eur. J.* **2011**, *17*, 117.

Graphic Abstract



Highlights:

- Two six-coordinate Co(II)-nitrate complexes are constructed by monodentate coordination mode.
- Static magnetic data and HF-EPR spectra demonstrate their easy-plane magnetic anisotropy.
- They display field-induced slow magnetic relaxation with the different relaxation mechanisms.